JOURNAL OF PROPULSION AND POWER
Vol. 18, No. 2, March–April 2002

Multilevel Analysis of Pulsed Detonation Engines

Houshang B. Ebrahimi*
Sverdrup Technology, Inc., Arnold Air Force Base, Tennessee 37389-6001
and
Rajendran Mohanraj† and Charles L. Merkle‡
University of Tennessee, Tullahoma, Tennessee 37388-9700

The present study explores some issues concerning the operational performance of pulsed detonation engines. Zero-, one-, and two-dimensional transient models are employed in a synergistic manner to elucidate the various characteristics that can be expected from each level of analysis. The zero-dimensional model provides rapid parametric trends that help to identify the global characteristics of pulsed detonation engines. The one-dimensional model adds key wave propagation issues that are omitted in the zero-dimensional model and helps to assess its limitations. Finally, the two-dimensional model allows estimates of the first-order multidimensional effects and provides an initial multidimensional end correction for the one-dimensional model. The zero-dimensional results indicate that the pulsed detonation engine is competitive with a rocket engine when exhausting to vacuum conditions. At finite back pressures, the pulsed detonation engine outperforms the rocket if the combustion pressure rise from the detonation is added to the chamber pressure in the rocket. If the two peak pressures are the same, the rocket performance is higher. Two-dimensional corrections added to the one-dimensional model appear to result in a modest improvement in predicted specific impulse over the constant pressure boundary condition.

Introduction

PULSED detonation engines (PDEs) are intermittent propulsive devices that produce a periodic impulse by detonating a fuel/oxidizer mixture placed inside one or more long narrow tubes that are closed on one end and open on the other. The cyclic process that describes the PDE operation comprises several parts. In the first, fuel and oxidizer are introduced into the tube through valves in the closed end or along the length of the tube. This injection process must ensure rapid and reasonably uniform mixing for a detonation to be sustained. As soon as the fresh charge of propellants fills the tube, a detonation is initiated from some point in the tube. This detonation sweeps through the tube converting the cold propellants to hot combustion products. Because the detonation propagates at a few kilometers per second, the resulting combustion process is accomplished at essentially constant volume conditions and provides a substantial pressure increase (nearly an order of magnitude) above the original pressure in the tube. After the propellants have been consumed, there follows a blowdown phase during which the hot, high-pressure gases are allowed to exhaust to ambient through the open end to produce the impulse that provides the propulsive thrust. This expansion process brings the tube back to its initial state, completing the periodic cycle. The ensuing propellant fill phase removes the residual hot gases as it again fills the tube with fresh propellant. In general, a region of buffer gases must be placed between the hot exhaust products and the newly entering propellant charge to prevent premature ignition or detonation.

The constant volume combustion process and the companion pressure increase generated by the detonation represent attractive attributes for any propulsion system. Because of these characteristics, PDEs have emerged as a possible alternative propulsion system for aircraft, missile, and rocket applications and are currently the recipient of considerable development effort.[1–8] As these implementations suggest, both airbreathing and nonairbreathing (rocketlike) versions of PDEs are envisioned. Many of the development issues associated with PDEs arise from the unsteady character of their flowfields.

Most of the corporate experience in the propulsion field has dealt with steady flow processes so that propulsion engineers are more conversant with steady flow analyses and measurements than with highly transient processes. The unsteady character of PDEs therefore represents a major departure. Although simple operational versions of a PDE can be easily constructed, the intermittent nature of the PDE renders the experimental measurement of performance considerably more complex than that of a companion steady flow device. Experimental measurements must provide high-frequency response with an absence of long-term drift to document the impulse generated during each pulse, even though the ultimate use of this information is to determine the time-averaged thrust. Similarly, the analytical techniques that are used to model the PDE are substantially different from the familiar steady flow tools that are used in most propulsion applications. The unsteady character of PDE operation makes computational fluid dynamics (CFD) analyses particularly attractive as a means for understanding the dominant characteristics of representative engine operation. Clearly the CFD analyses require careful experimental validation, but the inherent difficulties of making accurate measurements in this highly transient, wave-filled flow are also noted.

CFD analyses of PDEs represent only one aspect of a spectrum of analytical tools that are needed to provide guidance and evaluation during the development program, as well as to estimate their ultimate benefit. This spectrum of tools ranges from fast turn-around approximate analyses that can be used for preliminary design purposes to high-fidelity CFD tools that elucidate details of operation. In addition, the various analysis tools are useful for validating and/or providing corrections for each other while also providing guidance for companion experiments. The experiments, in turn, provide the ultimate validation of the analytical tools. In the present paper, we consider a spectrum of analytical tools of varying levels of fidelity to address the performance and operational characteristics of PDEs. Specifically, we consider zero-dimensional, one-dimensional, and two-dimensional analyses. All three levels of modeling involve unsteady processes, but require very different resources. A key goal

Received 22 September 2000; revision received 15 June 2001; accepted for publication 22 July 2001.

*Senior Research Engineer, Department of Computational Fluid Dynamics. Senior Member AIAA.
†Postdoctoral Research Associate, Department of Mechanical Engineering, current address Mississippi State University.
‡Professor, Department of Mechanical Engineering, H. H. Arnold Chair of Excellence in Computational Mechanics. Member AIAA.

is to integrate these different models in such a manner that they complement and augment each other.

A detailed assessment of PDE performance is necessary because of a continuing uncertainty in this area. Early estimates of specific impulses reported in the literature differed by more than a factor of two,[7] and, although these differences are being resolved, there remains some disagreement. One prime reason for the uncertainty in performance is simply because it is difficult to compare steady and unsteady processes on a common basis. A second major issue is that the manner in which the detonation pressure rise is incorporated into the cycle has a substantial impact on the performance relative to steady systems such as gas turbines or rockets. If the two systems are compared at the same peak pressure, the compression or pumping characteristics of the PDE can be reduced. This, of course, should give a weight and cost advantage to the PDE, but it does not give it a performance advantage. Alternatively, if the same pumping capability is included in both systems, the PDE will have a higher peak pressure that should transfer into an advantage in performance.

In the following sections we first outline the three levels of analyses and then give brief details of the zero-dimensional approximation along with corresponding results. We then present flowfield results from the two-dimensional analysis and use them to attempt a multidimensional end correction for the one-dimensional model. In the final section we estimate the performance corrections generated when this multidimensional end correction is used. Our analyses in the present paper are limited to single-tube operation under ideal conditions. Practical implementations of PDEs are expected to use multiple tubes manifolded together through common inlet and exhaust systems. CFD analyses appear particularly well suited for understanding the interaction between such multitube PDEs. Loss mechanisms include incomplete combustion due to partial mixing, effects of finite detonation initiation lengths, premature combustion arising because the incoming gases are preheated by the hot walls, and losses associated with valves, mixing, adjacent detonation tubes, and related issues.

Analytical Modeling of PDEs

The flow processes in a PDE are inherently unsteady in character and clearly require a transient analysis. The degree of fidelity of that analysis, however, depends on the particular features that are of interest. Certainly most phenomena have multidimensional features, but often the dominant effects can be replicated in a lower number of dimensions. Other processes require a fully three-dimensional analysis. For example, detonation initiation requires full three-dimensional effects, but the propagation of a detonation, and its pressure and temperature rise, can be accurately modeled in one dimension.[9] Thus, once the detonation is established, one-dimensional analyses become useful.

In a contrasting example, analysis of the detailed cell structure of a detonation also requires a three-dimensional model, but if this same three-dimensional analysis is extended to modeling the multipulse characteristics of a PDE, the computational requirements become impractical. The use of a lower-level model is mandatory if results are to be obtained in an acceptable time frame.

An important issue in PDE research is to identify those features that can be treated by the simpler analyses and those that require higher-level analyses. It is also important to estimate the errors incurred when simple models are used and to provide corrections where appropriate. For conventional, steady-flow engines, these tasks are currently well in hand. Similar understanding is necessary for PDEs. In the present study we contrast three different levels of analyses as a first step toward identifying the contributions that each can make to PDE development.

Zero-Dimensional Unsteady Model

The simplest model of a PDE is a zero-dimensional analysis in which the flow properties in the detonation tube are taken as uniform in space, but unsteady in time. This approximation is appropriate in the limit when the acoustic transit time through the detonation tube is small compared to the blowdown time.[10] In this limit, many acoustic waves pass through the tube before the mean quantities change appreciably. Although comparisons against a one-dimensional model are necessary to verify that both give similar results in the fast acoustic limit, the zero-dimensional analysis provides a useful first assessment of PDE operating characteristics. For selected conditions, it also allows closed-form solutions that provide much-needed pertinent functional dependencies. Under more general conditions, it requires only the integration of a single time evolution equation. These features make the zero-dimensional model appropriate for providing global understanding, and such a model should be useful in preliminary design applications where the interest is in comparing a large number of cases in a short time.

In the zero-dimensional approximation, the detonation propagates through the tube instantaneously so that the PDE cycle analysis simplifies considerably. The primary task in modeling the cycle then consists of simulating the blowdown from a chamber filled with burned products at high pressure. The fill process that prepares the chamber for the next detonation can be treated as an instantaneous process or as a second zero-dimensional process. In the present results, we consider only the blowdown step. Initial results of this nature have been previously presented by Talley and Coy,[10] and we follow their approach closely.

The zero-dimensional blowdown process is governed by the unsteady energy equation, which stipulates that the time rate of change of the total (extensive) internal energy in the chamber is equal to the product of the mass flow rate times the chamber enthalpy,

$$\frac{\mathrm{d}E}{\mathrm{d}t} = -\dot{m}h \tag{1}$$

Combining this relation with an appropriate equation of state and pertinent gas properties allows us to define the complete transient. For the equation of state, we choose the perfect gas law, $p = \rho RT$, and for ease of formulation, we use constant specific heats and a specified heat release. Although the constant properties cause the resulting predictions to be only qualitatively accurate, they can be calibrated by comparison with rocket engine predictions based on similar physics.

As long as the nozzle throat remains choked and the flow in the divergent section (if one is present) remains supersonic to the exit plane, it is possible to obtain a closed-form solution. The variation of chamber properties with time is obtained by assuming an adiabatic blowdown process. This yields the following expression for the speed of sound in the chamber at a given time:

$$c = c_i/(1 + \beta t) \tag{2}$$

where the time t is zero at the start of the blowdown process (just after the detonation wave reaches the exit), the subscript i denotes initial condition, and β is given by

$$\beta = \left\{[(\gamma - 1)/2][2/(\gamma + 1)]^{(\gamma + 1)/2(\gamma - 1)}\right\}(1/\tau) \tag{3}$$

where γ is the ratio of specific heats; τ, the characteristic blowdown time, is defined as $V/[A^*\sqrt{(\gamma RT_i)}]$; V represents the volume upstream of the throat; A^* is the throat area; T_i is the initial temperature in the chamber; and R is the gas constant. The chamber properties can be expressed in terms of c/c_i from Eq. (2). The impulse I and the total mass outflow m from the chamber can be expressed as

$$I = \frac{2}{\gamma + 1} p_i A^* \tau \frac{1 + \gamma M_e^2}{M_e\left\{1 + [(\gamma - 1)/2]M_e^2\right\}^{\frac{1}{2}}} \times \left\{1 - (1 + \beta t)^{-(\gamma + 1)/(\gamma - 1)}\right\} - p_\infty A_e t \tag{4}$$

$$m = (p_i/RT_i)V\left\{1 - (1 + \beta t)^{-2/(\gamma - 1)}\right\} \tag{5}$$

For the special case of a thruster exhausting into vacuum, the pressure–area terms disappear, the outflow remains supersonic for all time, and, at the infinite blowdown time limit, the specific impulse $I_{sp} = I/(mg)$, where g is the acceleration due to gravity, has

a simple form. Denoting this value by I_{sp-tr} and the corresponding value for the steady-state rocket by I_{sp-ss}, we have

$$I_{sp-tr}/I_{sp-ss} = [2/(\gamma+1)]\sqrt{T_i/T_c} \tag{6}$$

where T_c is the temperature in the conventional rocket chamber. Note that T_c is lower than T_i. The temperature of products after detonation has swept through because the detonation process results in a higher temperature than that which is obtained with constant pressure combustion. This result [Eq. (6)] holds for converging–diverging nozzles of any expansion ratio. The first term is clearly less than unity, whereas the square root term is larger than unity because the temperature behind the detonation, T_i, is larger than that in the rocket, T_c (assuming the same propellant ratio). Overall, the product of these two quantities is near unity, implying that the specific impulses of the two systems at vacuum are comparable. Thus, at zero backpressure, where the chamber pressure does not impact the specific impulse, the performance of the PDE does not exceed that of a conventional rocket engine.

At finite backpressures, the specific impulse does depend on the chamber pressure, and the relative performance of the two engines may be expected to differ. In addition, finite backpressure complicates the analysis because the flow in the nozzle can now become subsonic. For the unsteady case for which the chamber pressure decreases with time, any finite backpressure will eventually lead to subsonic (and unchoked) flow if the expansion is allowed to continue for a sufficient time. For the steady case, the first appearance of subsonic flow will depend on the nozzle expansion ratio and the chamber to backpressure ratio. Although the preceding-closed-form equations could, in principle, be extended to this more general case, it is easier to integrate the energy equation directly by numerical means.

For purposes of numerical solution, the energy equation can easily be manipulated to give a differential equation for pressure:

$$\frac{\mathrm{d}p}{\mathrm{d}t} = -\frac{\sqrt{\gamma RT_0}}{V}\frac{\gamma pAM}{\sqrt{T_0/T}}$$

In this expression, T_0 is again a constant and the remaining pressure and temperature terms are evaluated at chamber conditions, whereas the area and the Mach number are evaluated at the throat. As long as the exit plane remains supersonic, the numerical results duplicate the closed-form solution. Once a shock wave appears in the nozzle, the results start to differ. The shock wave appears at the exit plane when the chamber pressure drops to the point where a shock at the nozzle exit just causes the exit pressure to reach the ambient pressure. This starts the propagation of the shock through the nozzle to the throat, at which time the nozzle unchokes and the mass flow starts to decrease.

Representative results obtained from the numerical solution of the zero-dimensional equation are summarized in Figs. 1 and 2 for two contrasting sets of conditions. Figures 1 and 2 present the specific impulse of both systems as a function of nozzle expansion ratio for a series of backpressures. Five different backpressures are considered: vacuum, 0.01, 0.1, 0.2, and 0.5 atm. The corresponding chamber pressures are either 10 or 1.25 atm as noted hereafter. In both cases, the specific impulse assumes that the oxidizer is carried on board.

Figure 1 shows the specific impulse for both systems for the case where the initial pressure is the same in both the PDE and the rocket (10 atm) whereas the temperature in the PDE is 20% higher than that in the rocket (2800 vs 2330 K). This case corresponds to the situation in which the pump used in the PDE involves a lower pressure rise than that in the rocket so that the peak pressures in both systems are comparable. The higher initial temperature for the PDE is indicative of the difference between a detonation and a deflagration. The results on Fig. 1 show that at vacuum conditions, the two systems give nearly identical performance, in agreement with the closed-form result. At finite backpressures, the rocket I_{sp} always exceeds that of the PDE.

The results in Fig. 2 simulate conditions where pumps involving the same pressure size are used in both engines. The combustion pressure rise is used to raise the peak pressure in the PDE above that in the rocket. Here we have used a factor of eight for this ratio. The initial PDE pressure is again 10 atm, whereas the rocket

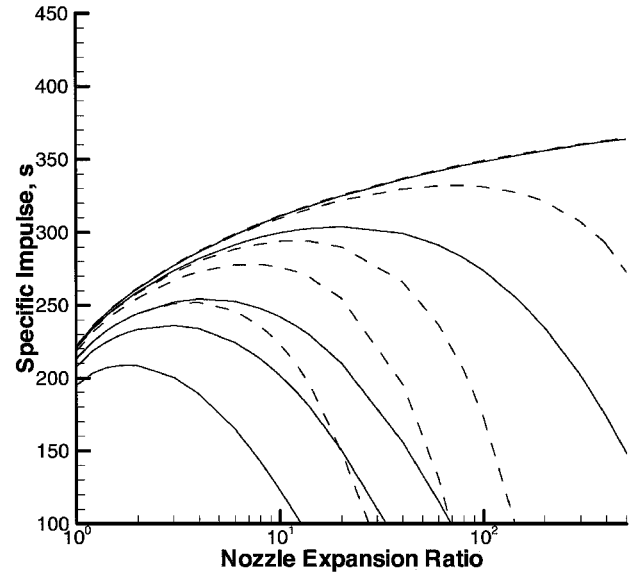

Fig. 1 Comparison of specific impulse for PDE and steady-state rocket based on zero-dimensional analysis: $p_i = p_c = 100{,}000\ \mathrm{N/m^2}$, $T_i = 2800\ \mathrm{K}$, $T_c = 2330\ \mathrm{K}$; curves starting from the top represent vacuum, $1000\ \mathrm{N/m^2}$; $10{,}000\ \mathrm{N/m^2}$; $20{,}000\ \mathrm{N/m^2}$; and $50{,}000\ \mathrm{N/m^2}$, respectively (——, PDE and – – –, steady-state rocket).

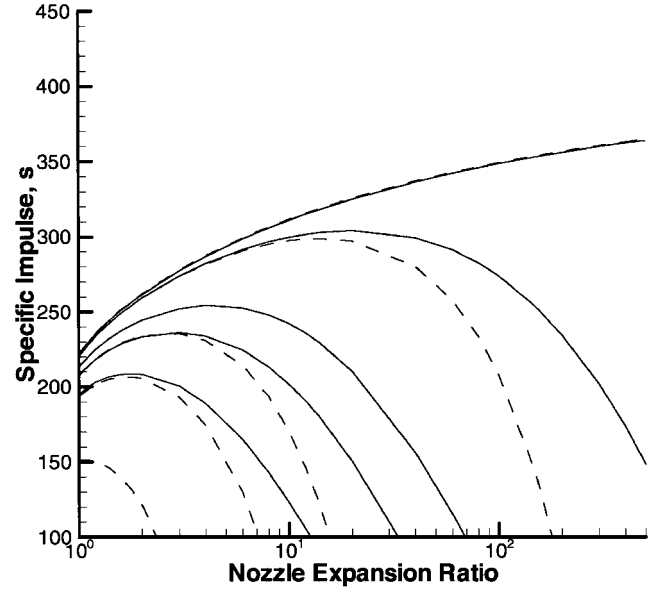

Fig. 2 Comparison of specific impulse for PDE and steady-state rocket based on zero-dimensional analysis: $p_i = 100{,}000\ \mathrm{N/m^2}$, $p_c = 12{,}500\ \mathrm{N/m^2}$, $T_i = 2800\ \mathrm{K}$, $T_c = 2330\ \mathrm{K}$; curves starting from the top represent vacuum, $1000\ \mathrm{N/m^2}$; $10{,}000\ \mathrm{N/m^2}$; $20{,}000\ \mathrm{N/m^2}$; and $50{,}000\ \mathrm{N/m^2}$, respectively (——, PDE and – – –, steady-state rocket).

chamber pressure is 1.25 atm. As before, the temperatures are 20% apart. Comparison with Fig. 1 verifies that the results at the vacuum condition are unchanged by the change in pressure, and the two systems again give nearly identical performance at vacuum conditions. The impulse for the PDE at finite backpressures, however, is now substantially higher than that for the rocket.

Comparing the results in Figs. 1 and 2, we note that the monotonically decaying pressure in the PDE results in an average pressure that is lower than its initial value. Consequently, unless the PDE starts at a substantially higher pressure than the rocket, it will provide lower performance at finite backpressures. The advantage of the detonation is that it provides sufficient pressure rise to allow improvement.

The zero-dimensional results give a quick overview of the comparative performance of the PDE and the rocket. The key issues relate to the reliability of the zero-dimensional approximation, the potential effects of multipulse operation at various periods, and the differences that are encountered as the complexity of the model is increased. The next logical step is the introduction of a one-dimensional model. Our initial one-dimensional results suggest that wave dynamics continue to have an impact on PDE performance as the acoustic time is shortened, but definitive comparisons are not yet available. Because one-dimensional results have been previously reported elsewhere,[11,12] we here turn directly to the two-dimensional solutions. We then return to the one-dimensional model and assess the impact that these two-dimensional results have on the one-dimensional solutions.

Two-Dimensional Flowfield Modeling

Multidimensional effects are present in nearly every aspect of PDE operation. As noted earlier, however, a full multidimensional analysis of the entire PDE cycle under periodic conditions (which requires the computation of several cycles to ensure that periodic conditions have been reached) is computationally very intensive. It is, nevertheless, crucial to attempt to identify those key processes that are inherently multidimensional, causing the one-dimensional approximations to be severely impaired.

In the past, Ebrahimi and Merkle have addressed several such multidimensional effects.[13] The results show that most of these multidimensional phenomena have little impact on the global characteristics of the results. For example, the effects of initiating the detonation in a two-dimensional manner are largely obliterated as the detonation rapidly approaches a globally one-dimensional character. Similarly, the effect of including internal geometry variations in the head end region again has little influence on the overall propagation of the detonation. Finally, the presence of heat conduction from the walls during the fill process does not lead to significant precombustion in our simulations.

In the present paper we consider the significance of multidimensional expansion at the open end and extend these findings to our one-dimensional model to provide an assessment of how multidimensional corrections can be incorporated into a one-dimensional model. We first present the two-dimensional results and then turn to their one-dimensional implications.

Two-Dimensional Effects at an Open End

The classical constant pressure boundary condition at an open end is clearly only an approximation to the complete multidimensional effects that are encountered when a disturbance reaches the end of a tube. The most appropriate way to treat this boundary is to include the external region in the computational domain so that the open end becomes an internal part of the computational domain.[4,14] To assess the degree to which this simplified boundary condition impacts one-dimensional predictions, we present some representative two-dimensional computations that include a large external region outside the detonation tube in addition to the internal region. The external portion of the computational domain allows us to capture the approximately cylindrical shock wave that is generated when the detonation arrives at the open end of the tube. The two-dimensional solutions produce a nearly one-dimensional flowfield inside the detonation tube, but the propagation of the shock wave in the external domain changes the local pressure around the tube opening substantially in the initial time following the arrival of the detonation. The detonation sets up an external shock wave that initially starts as a planar wave over the tube area, but begins to approximate a cylindrical shock as it propagates away from the nozzle exit plane.

The computational domain and the detonation tube geometry used for the two-dimensional results reported herein are given in Fig. 3. Because our focus is on the effects of external conditions on the internal flowfield, we use a relatively short detonation tube of 102 mm in length by 20 mm high. (Results for an even shorter tube are presented elsewhere.[13]) As Fig. 3 indicates, the external domain was approximately four times the length of the tube (380 mm in length by 560 mm high) to enable computations to be extended for a reasonable time. The detonation tube was approximately centered in this external domain (see Fig. 3). The top-to-bottom symmetry about the midplane was used to reduce computational costs. A uniform grid of nominally 0.4 mm was used inside the tube with slightly smaller sizes near the exit plane. The external grid used cells of approximately 1.0 mm near the tube boundaries with mild stretching toward larger sizes in the upstream and downstream directions.

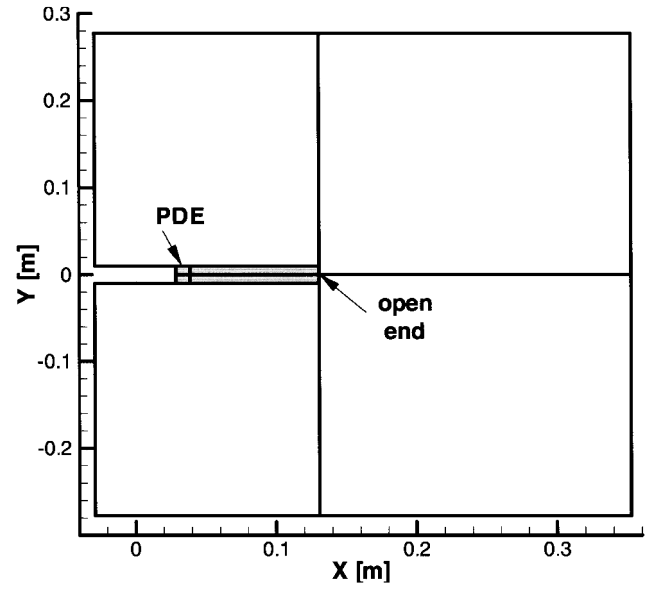

Fig. 3 Computational domain and detonation tube geometry for two-dimensional exit-plane study.

A brief critique of this isolated PDE problem depicted in Fig. 3 places the resulting observations in context. The isolated detonation tube is clearly not a practical situation. Most PDE installations would be composed of several detonation tubes clustered together, so that each tube would have near neighbors whose exhaust would impact each other. Similarly, the PDE installation would almost certainly be adjacent to a vehicle surface that would also reflect the external wave back onto the tube exit. Finally, the external domain only impacts the internal flowfield when the flow exiting the detonation tube remains unchoked. As noted in the zero-dimensional results, it is imperative to operate PDEs at pressure levels at least as high as those used in conventional engines so that the percentage of time spent with unchoked outflow will likely be small. Nevertheless, the present calculations serve to estimate the approximate impact that multidimensional effects at the exit plane could have in this idealized situation.

The detonation in the two-dimensional calculations was initiated by a high-pressure/temperature region 10 mm in length that extended across the entire tube cross section. The initial temperature in this region was 3000 K, and the initial pressure was 30 atm. Initial conditions in the remainder of the domain (external and internal) were 300 K and 1 atm. The internal fluid was taken as a stoichiometric mixture of hydrogen and oxygen, and the external environment was taken as pure oxygen. The two-dimensional simulation corresponds to a first-pulse detonation in the tube with quiescent initial conditions throughout the domain. In the periodic case, the fluid inside the tube would have residual motion and pressure gradients from the previous pulse, and the environment outside the tube would also contain disturbances.

The computation was stopped just after the external shock reached the outer boundary. The total time simulated was approximately 0.45 ms and extended just beyond the time at which the flow at the PDE exit plane reversed from outflow to inflow. At this time, the external shock was some 35 tube half-heights away from the PDE exit plane in downstream, upstream, and transverse directions. We note that the 0.45-ms time is short in comparison with practical PDE cycle times of nominally 100 pulses per second (10-ms period).[6,8] Nevertheless, it represents a compromise between simulating the dominant physics and maintaining practical computation times.

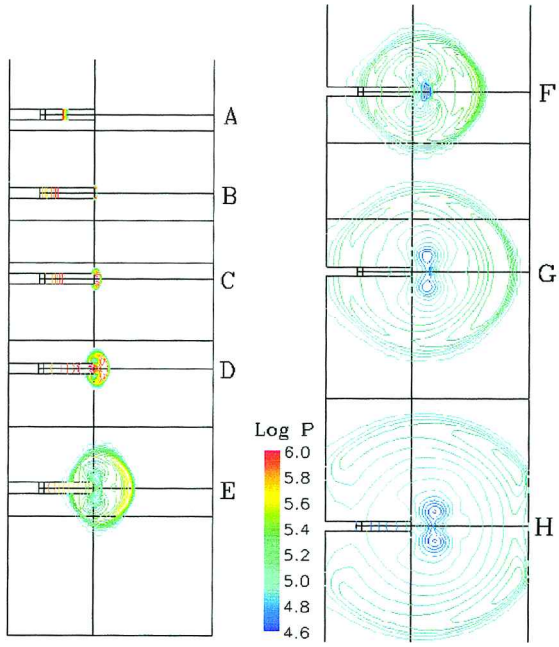

Fig. 4 Time history of Mach number contours with viscous effects and finite rate chemistry.

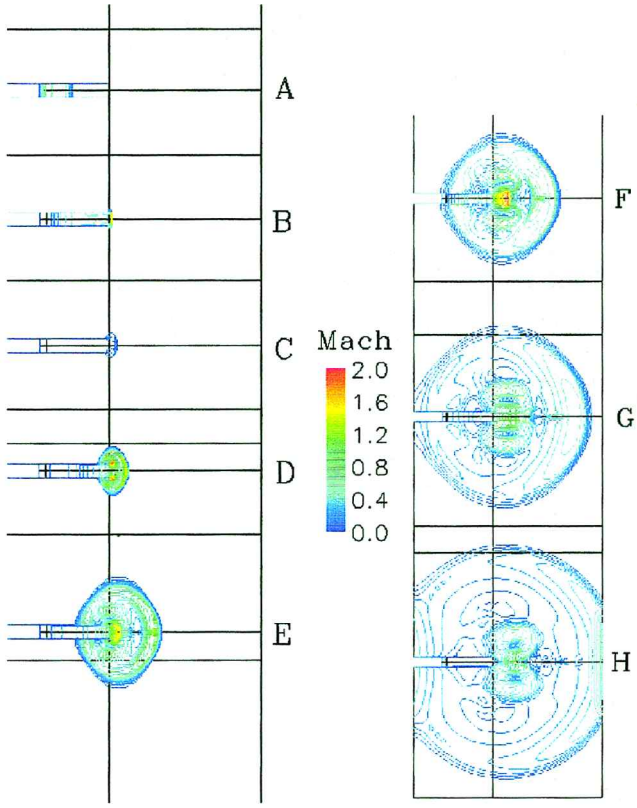

Fig. 5 Time history of pressure contours with viscous effects and finite rate chemistry.

The two-dimensional computations included complete hydrogen–oxygen kinetics. Further details of the computational method are given in Ref. 15.

Two-Dimensional Results

Figures 4 and 5 show Mach number and pressure contours in both the internal and external fields for a sequence of eight time instants. In the first frame the detonation is approaching the end of the internal tube whereas in the last the external shock has just reached the outer boundary. As noted earlier, the computation corresponds to an initial pulse. The results of this initial pulse enable easier interpretation of events and require a much smaller computational domain and computer time compared to a multiple-pulse case. The same contour levels are used in all frames so that the decay of the peak values with time is visible.

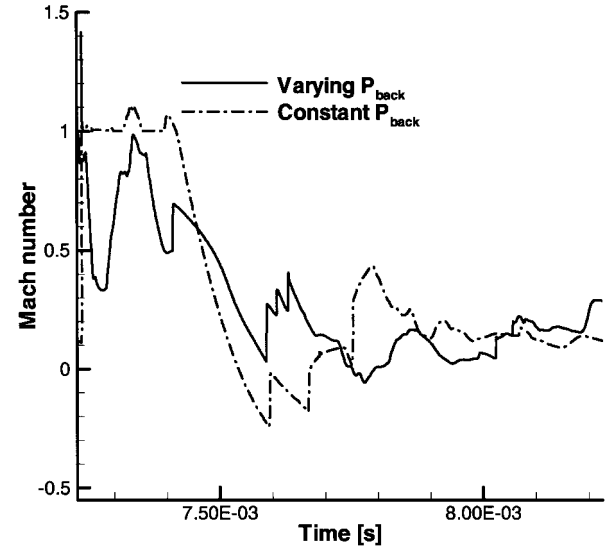

Fig. 6 Exit Mach number for periodic operation; solid line corresponds to time-varying backpressure, dashed line corresponds to constant backpressure.

Frame A of Figs. 4 and 5 shows the Mach number and pressure contours before the detonation has reached the end of the open tube. These solutions at this time instant are in good agreement with a one-dimensional computation and show the characteristic features common to such solutions.[4,6,7]

Frame B of Figs. 4 and 5 shows conditions just after the detonation has emerged from the tube. Because the ambient gas contains no fuel and the burned gas is stoichiometric, the detonation decays to a shock wave as it moves outside the tube. The shock wave is highly curved and nearly cylindrical at the top and bottom edges of the tube whereas the remainder of the shock front is nearly planar. In frame B, we see the first deviations from a classical one-dimensional solution. The pressure inside the shock is much higher than ambient, and so the velocity at the exit plane is subsonic over the entire passage. In the one-dimensional approximation based on the constant pressure boundary condition, the exit Mach number instantaneously reaches the sonic value when the detonation reaches the exit and stays choked until the internal pressure decays sufficiently (discussed later and illustrated in Fig. 6). In the two-dimensional solution, the Mach number profile behind the detonation remains almost unchanged when the detonation reaches the exit because the external compression is similar to that observed inside the tube. The only region in which the two-dimensional Mach number reaches the sonic velocity is in a very small region near the upper and lower corners where the flow is essentially expanding in shock-tube fashion.

In frames C and D, the external shock has progressed appproximately one-half and one tube heights away from the exit plane, respectively. Again the flow remains subsonic over most of the exit plane, and the pressure at the exit plane remains much above the ambient level. These frames also show that the shock is traveling forward along the outside of the tube and enveloping the exit plane to shield it from external conditions. The essentially planar shock shape in frame B is now approaching a cylindrical shape. As the shock distance becomes much larger than the tube height, the external shock spreads in all directions, similar to a shock created from the point source. However, a noteworthy contrasting feature is the directivity associated with the shock strength, which is maximum along the extended axis of the detonation tube.

In frames E and F, the shock has traveled approximately one and one-half and two tube heights past the exit plane. Note that it has

propagated a similar distance in the directions normal to the tube and back upstream along the outer surface. The effects of the outflow from the tube, however, are maintaining a stronger shock in the downstream region than in the transverse and upstream regions. Again, the Mach number at the exit plane remains subsonic across the entire duct. There are two supersonic regions on the centerline, but they are both downstream of the exit plane. Detailed inspection of the pressure inside the tube indicates that the entire tube and all of the gas inside the shock is at a pressure that is substantially above ambient (around 6 atm). It is the presence of this high pressure outside the tube that keeps the outflow subsonic. Although these observations are quite different from a corresponding one-dimensional result, we do note that the present plot corresponds to a very early time in a PDE cycle and that the time interval represented by these frames will be a small fraction of a typical time period.

As time increases, the shock continues to propagate outward. The pressure immediately behind the shock decreases slowly with time as the shock weakens because of the two-dimensional expansion, but the pressure near the exit plane decreases rapidly because the gas is moving radially outward. Representative Mach number contours for a time at which the shock has traveled about two and one-half tube heights are given in frame G. At this time, the pressure outside the exit has decreased to approximately two atmospheres, but the outflow remains subsonic. Nevertheless, the Mach number at the exit plane is increasing slowly. The Mach number on the centerline outside the tube shows very strong axial gradients resulting from the cylindrically expanding shock wave.

The final frame given in Figs. 4 and 5 again shows subsonic flow at the exit plane, but in the interim between frames G and H, the exit flow has gone supersonic (to about $M = 1.2$) across the entire duct exit plane. It is now rapidly decreasing and will soon reach inflow conditions. The pressure at the exit plane of the tube has actually decreased below ambient pressure, but the flow remains outward because the pressure outside the tube is even further below ambient. Also note that at this time the external flow has propagated all of the way to the upstream end of the tube, and there is a wide zone of flow going in the upstream direction. This external flow will gradually decay, but significant disturbances will likely remain beyond the time for the next PDE pulse. This will result in detailed changes in the interaction between the external surface of the tube and the external environment. Perhaps more importantly, the present computations imply that the detonation tube is isolated in space and that there are no external surfaces (from a vehicle or a second detonation tube) that would disrupt this external shock and reflect it back toward the exit plane.

Multidimensional End Corrections for One-Dimensional PDE Analyses

As a means of incorporating the leading-order multidimensional end corrections into a one-dimensional model, the two-dimensional solutions have been used to specify a temporally varying pressure at the exit plane. For this the pressure across the exit plane was averaged at each instant of time and used as a time-varying boundary condition for the one-dimensional problem. Throughout the two-dimensional computation, the pressure at the exit plane remained nearly uniform across the tube except for the gradients at the outer edges noted earlier. The average pressure, therefore, is approximately equal to the local pressure over most of the tube cross section, suggesting that an averaging process is reasonable. Furthermore, the flow inside the tube remained essentially one-dimensional throughout the solution. The combination of a nearly uniform pressure and approximately one-dimensional internal flow suggests that the pressure boundary condition should incorporate many of the two-dimensional effects into the one-dimensional model. In addition, comparisons between one-dimensional solutions based on the spatially averaged pressure and the centerline value were in close agreement, further supporting this conclusion.

The lengths of the tube and the detonation initiation region in the one-dimensional domain were chosen identical to those used in the two-dimensional computation to make the two results as similar as possible. One difference between the two computations, however, was that the two-dimensional results included complete chemical kinetics effects, whereas the one-dimensional model used a single-step, global model. This difference appeared to introduce some variation in the acoustic transit times through the tube as is noted later.

Because the two-dimensional computations were only for a first-pulse condition and extended for only 0.45 ms, a mathematical continuation was required to specify the downstream boundary condition over the entire cycle. As a means of generating a smooth transition from the final pressure in the two-dimensional solution back to the ambient pressure, we added an exponential function to the end of the two-dimensional results. The time constant used in this exponential relaxation was varied, and a series of computations was made where only a portion of the two-dimensional solution was enforced as a boundary condition to test the sensitivity to this extrapolation procedure. For multipulse computations, this extended pressure–time signal was replicated in periodic fashion to each successive pulse in the computation. One-dimensional predictions based on this time-varying backpressure were obtained for several different PDE cycle times to ascertain effects of varying the period. For all solutions, a constant pressure boundary condition was used as a reference case.

The spatially averaged pressure taken from the two-dimensional solution is given in Fig. 7 along with the exponential relaxation function with a characteristic relaxation time of 0.1 ms. The two-dimensional portion of the curve lies on the left side of Fig. 7 between $t = 0$ and 0.45 ms. The remainder of the curve shows the exponential relaxation back to ambient conditions.

Figure 7 clearly shows that the pressure jumps to approximately 10 atm as soon as the shock emerges from the tube. For approximately the next 0.3 ms the exit pressure remains higher than ambient because of the effect of the expanding external shock (seen in Figs. 4 and 5), although it is decreasing rapidly during this time interval. For the remainder of the two-dimensional computation, the pressure is below the atmospheric pressure. For convenience, we refer to this as the suction phase. At the end of the two-dimensional solution ($t = 0.45$ ms), the pressure at the exit plane is at approximately 0.7 atm, although as Fig. 7 shows, a minimum pressure has been reached and the pressure is slowly starting to increase again. We note that the flow at the exit plane does not reverse and generate inflow until approximately 0.40 ms, a considerable time after the pressure has dropped below the atmospheric level.

The relaxation portion of the curve shown on Fig. 6 (time constant 0.1 ms) appears to be a reasonable choice. The exponential curve smoothly brings the pressure back to ambient before the end of the

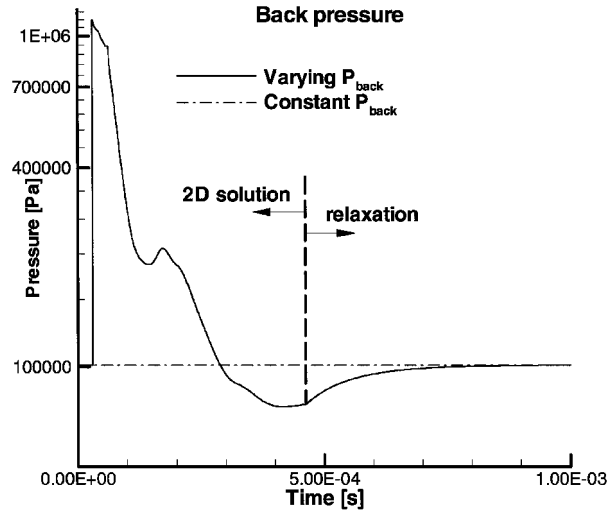

Fig. 7 Time-varying exit pressure boundary condition used to simulate multidimensional end correction in one-dimensional solution. Left portion ($t < 0.45$ ms) represents results obtained from the two-dimensional solution; right portion represents exponential relaxation back to ambient. Time constant, 0.1 ms; period, 1 ms; and ambient pressure, 1 atm.

period. Note that for the longer cycle times (2 and 5 ms) this same exponential curve was followed, so that the pressure was essentially atmospheric for the lengthened portions of the cycle. Several alternative extrapolation conditions were tested. Results are presented hereafter from computations with a relaxation time of 0.01 ms (the extended curve transitions rather abruptly from the two-dimensional result to ambient conditions) and with the two-dimensional solution terminated at the point where the pressure first reduces to the ambient value and is taken as constant from there on, that is, there is no suction phase.

As a first indication of the effect of the time-varying (two-dimensional) boundary condition on the solution, we present the exit Mach number variation throughout a period for the two cases. These results are for a cycle time of 1 ms, and the detonation tube is operating under periodic conditions. There are two major differences between the two curves. First, the constant pressure case remains choked for approximately the first 0.3 ms of the cycle, whereas the time-varying backpressure case becomes sonic for only an instant. The reason is that the detonation raises the pressure at the exit plane by a substantial amount (refer to Fig. 7). Including the effects of the external shock increases the pressure immediately outside the tube, and so the flow stays subsonic in the varying pressure case. By contrast, enforcing the ambient pressure when the exit pressure is this high forces the flow to choke. The second effect is that the constant pressure solution shows a long period of reverse flow whereas the varying pressure shows only a momentary flow reversal. This again is a direct result of the suction pressure region in the two-dimensional solution.

The effect of these two different boundary conditions on the I_{sp} gives an effective integrated measure of their importance to the overall cycle. A comparison of the specific impulse computed from these two one-dimensional solutions is given in Fig. 8 for three different cycle times, 1, 2, and 5 ms. There are four curves shown in Fig. 8. The bottom two are the cases of main interest. The ambient pressure boundary condition results in the lowest specific impulse. At all three periods, the varying (two-dimensional) backpressure results in an improvement of approximately 3–5%.

The remaining two curves in Fig. 8 offer additional insight into this varying backpressure effect. The first of these two curves corresponds to the two-dimensional backpressure with a faster relaxation time (characteristic time 0.01 ms). This relaxation curve terminates the suction region almost immediately after the two-dimensional portion of the curve and returns the pressure to the ambient value. The final result in Fig. 8 is for a computation that has no suction region at all. As soon as the two-dimensional solution reaches ambient pressure level, it is replaced by a constant ambient pressure condition for the remainder of the cycle. The results in Fig. 8 show a monotonic increase in I_{sp} with a decrease in suction pressure (apart from the constant ambient pressure case). This is at first surprising because reducing the pressure below ambient decreases the amount of reverse flow. (This can be verified by comparing exit Mach number curves.) The difference, however, is that the subatmospheric pressure on the exit plane corresponds to a pressure drag that causes a thrust penalty just like the momentum inflow (which occurs when the exit pressure equals ambient) does.

We emphasize that the 0.1-ms relaxation case in Fig. 8 is the most justifiable. It appears to be a better extrapolation of the two-dimensional solution than the 0.01-ms case, and it uses all of the two-dimensional results whereas the zero-suction curve omits part of them. As noted, the two-dimensional effects appear to have a modest positive effect on I_{sp}. (Note that in steady flow, multidimensional effects almost always decrease I_{sp}.) We also remark that the results of a series of additional one-dimensional computations with minor changes in the parameters suggest that the effects of the two-dimensional boundary condition are quite sensitive to getting everything right. Changing the percent fill when the varying pressure is used has a larger effect on I_{sp} than when constant pressure boundary conditions are used. (The present results represent conditions where the tube is essentially 100% filled with propellants at detonation arrival. Previous results[11] indicate that partial filling improves I_{sp} in many cases, although it simultaneously decreases thrust.) The added sensitivity to fill ratio appears to be such that, when, the tube is partially filled, the detonation decays to a shock before it emerges from the tube, and the initial overpressure is much smaller than observed in the present full-tube detonations. Consequently, the variable pressure boundary condition should be scaled to reflect this weaker disturbance. In addition, one-dimensional results indicated that the application of the varying pressure conditions resulted in more rapid change in the I_{sp} when the length of the initiation region was changed.

As a final check on our end correction, we compare results for the exit Mach number for the one-dimensional solution with that from the two-dimensional solution. To keep the comparison as meaningful as possible, we do this comparison for the first pulse condition. The results are given in Fig. 9. Comparing first the one-dimensional solution with the two-dimensional results, we see that the two dimensional solution remains choked for approximately twice as long as the one-dimensional result based on the two-dimensional

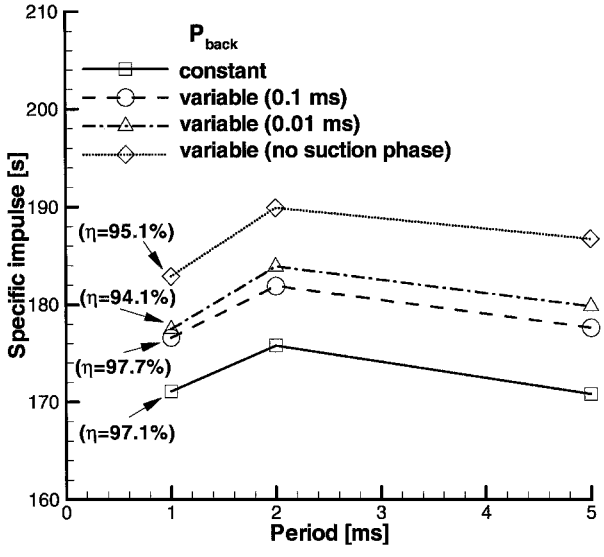

Fig. 8 Comparison of time-varying and steady boundary conditions on specific impulse as a function of cycle time; the value of η denotes the percentage of fuel burnt and is indicated when it is below 100% (this occurs for 1.0-ms period for all cases) due to unreacted propellants exiting the chamber.

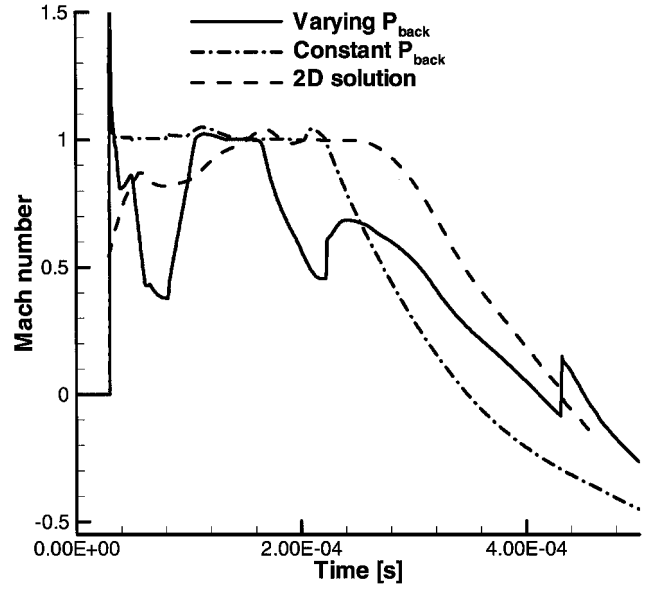

Fig. 9 Comparison of exit Mach number of first pulse solutions for constant pressure case, varying pressure case, and two-dimensional solutions.

boundary condition. By coincidence, it is seen that the constant pressure boundary condition results in nearly the same length of choked flow as the two-dimensional solution. We also clearly note that the constant pressure solution chokes as soon as the detonation arrives, whereas the variable pressure solution and the two-dimensional solution remain subsonic for some time before choking.

The differences between the two-dimensional solution and the one-dimensional solution with a time-varying boundary condition are somewhat surprising, but inspection of the one-dimensional result indicates that the difference is because of conditions inside the tube. It is clear that an expansion wave reaches the exit and causes the flow to unchoke in the one-dimensional case. This expansion wave is absent in the two-dimensional case. Comparisons with other two dimensional results (not shown) for a slightly shorter tube (6 mm) shows that the exit Mach number is quite sensitive to conditions inside the tube. The two-dimensional results for the shorter tube choked only momentarily, not for several tens of microseconds as in the present case. It is speculated that the different chemistry models used in the one- and two-dimensional solutions result in a change in the wave transit time that makes the effective length of the one-dimensional tube appear shorter. Finally, by referring to the periodic Mach number solutions in Fig. 6, we note that the difference between the periodic case and the first pulse is also quite large. The Mach number variation for the periodic case is (like the shorter tube two-dimensional case) choked only momentarily. Thus, the periodic solution is very different from the first-pulse two-dimensional solution. This suggests that some care must be exercised in creating a general multidimensional correction for one-dimensional solutions. Nevertheless, the overall effect of multidimensional effects performance is seen to be relatively small for the cases studied, and the specified pressure condition appears to be a reasonable way to correct for multidimensional effects.

Conclusions

Three different levels of analysis have been used to investigate the characteristics of PDEs: zero dimensional, one dimensional, and two dimensional. These multiple approaches provide complementary understanding and mutually support each other. The zero-dimensional results indicate that at vacuum conditions where the specific impulse depends only on the temperature, the effects of the constant volume combustion provide no advantage, and the performance of PDEs is essentially identical to that of a rocket engine. At finite backpressures, the conclusions are more interesting. When the peak pressure in the PDE is equal to that in the rocket, its I_{sp} is considerably lower than that of the rocket. If the entire detonation pressure rise is added to the chamber pressure of the rocket, the conclusion reverses and the PDE provides considerably better performance. In general, the two systems become competitive at some intermediate condition. Preliminary one-dimensional analyses at conditions where the fast acoustic limit of the zero-dimensional approximation applies suggest that some residual wave effects still remain, but additional work is needed to quantify this observation.

Two-dimensional computations that include a large external domain show that the local pressure near the exit plane fluctuates dramatically as the detonation emerges from the tube and generates a shock in the external field. The local pressure initially rises to around 10 atm (for 1.0 atm ambient pressure) before falling to nearly 0.7 atm as the shock recedes. The initial high-pressure region delays choking at the exit for some time, whereas the subatmospheric pressure delays flow reversal. In general, however, both choking and flow reversal occur. The duration of either of these conditions is influenced by interactions between the internal and external fields.

As a means of testing the sensitivity of the open-end boundary condition in a one-dimensional analysis to multidimensional effects, a time-varying backpressure was obtained from the two-dimensional results. One-dimensional computations using this boundary condition were then compared with solutions based on a constant pressure condition. The results indicate that I_{sp} is improved by 3–5% when the simulated two-dimensional boundary condition is used. Experiences from a number of one-dimensional computations of this type suggest that the increment in performance is relatively sensitive to the precise pressure distribution used. In particular, care must be used to discern between an initial pulse and a periodic pulse to be sure that performance is not stolen from adjacent cycles.

Practical PDE installations will not allow an isolated detonation tube without nearby surfaces or adjacent tubes. Consequently, the present isolated two-dimensional solution gives only an indication of the level of interference that can be expected. The implications are that major interference will not be experienced apart from the obvious problems that occur if tuning is incurred between components. Finally, we note that both the zero- and one-dimensional results indicate that elevated chamber pressures are desirable. This implies that the exit boundary will be choked over large fractions of the cycle and will minimize these external interactions.

Acknowledgment

This work was supported by NASA Marshall Space Flight Center under Contract NAS8-97301. Valuable discussions with Robert Heirs of Arnold Engineering Development Center are gratefully acknowledged.

References

[1]Eidelman, S., and Grossman, W., "Pulsed Detonation Engine Experimental and Theoretical Review," AIAA Paper 92-3168, Jan. 1992.

[2]Bussing, T., and Pappas, G., "Pulse Detonation Engine," AIAA Paper 95-2577, July 1995.

[3]Lynch, D., Edelman, R., and Palaniswamy, S., "Computational Fluid Dynamics Analysis of the Pulse Detonation Engine Concept," AIAA Paper 94-0264, Jan. 1994.

[4]Cambier, J. L., and Tegner, J. K., "Strategies for Pulsed Detonation Engine Performance Optimization," *Journal of Propulsion and Power*, Vol. 14, No. 4, 1998, pp. 489–498.

[5]Eidelman, S., Grossmann, W., and Lottati, I., "Review of Propulsion Applications and Numerical Simulations of the Pulse Detonation Engine Concept," *Journal of Propulsion and Power*, Vol. 7, No. 6, 1991, pp. 857–865.

[6]Bratkovich, T. E., and Bussing, T. R. A., "Pulse Detonation Engine Performance Model," AIAA Paper 95-3155, July 1995.

[7]Kailasanath, K., Patnaik, G., and Li, C., "Computational Studies of Pulse Detonation Engines: A Status Report," AIAA Paper 99-2634, June 1999.

[8]Brophy, C. M., and Netzer, D. W., "Effects of Ignition Characteristics and Geometry on the Performance of a JP-10/O_2 Fueled Pulse Detonation Engine," AIAA Paper 99-2635, June 1999.

[9]Khoklov, A. M., and Oran, E. S., "Deflagrations, Hot Spots, and the Transition to Detonation," AIAA Paper 99-3771, June 1999.

[10]Talley, D., and Coy, E., "Constant Volume Limit of Pulsed Propulsion for a Constant γ Ideal Gas," AIAA Paper 2000-3216, July 2000.

[11]Mohanraj, R., and Merkle, C. L., "Numerical Study of Pulse Detonation Engine Performance," AIAA Paper 2000-0315, Jan. 2000.

[12]Mohanraj, R., Ebrahimi, H. B., and Merkle, C. L., "Pulse Detonation Rocket Engines," *Proceedings of the Fourth International Symposium on Liquid Space Propulsion*, Heilbronn, Germany, March 2000.

[13]Ebrahimi, H. B., and Merkle, C. L., "Numerical Simulation of the Pulse Detonation Engine with Hydrogen Fuels," AIAA Paper 99-2259, June 1999.

[14]Li, C., Kailasanath, K., and Patnaik, G., "Numerical Study of Flowfield Evolution in a Pulsed Detonation Engine," AIAA Paper 2000-0314, Jan. 2000.

[15]Ebrahimi, H. B., and Kawasaki, A., "Numerical Investigation of Exhaust Plume Radiative Transfer Phenomena," AIAA Paper 98-3623, July 1998.